Semesta Teknika
Vol. 28, No. 1, 47-61, May 2025
DOI: https://doi.org/10.18196/st.v28i1.25841

Evaluating Flow Resistance in Straight Channels Using 2-Point Velocity Measurements

Ali Nursamsi Dahlan, Bambang Agus Kironoto*, Adam Pamudji Rahardjo
Department of Civil Engineering, Universitas Gadjah Mada, Yogyakarta

[1] Jl. Grafika No.2, Sendowo, Sinduadi, District. Mlati, Sleman Regency, Yogyakarta, Indonesia

* Corresponding author email: kironoto@ugm.ac.id

Keywords:
Manning, Composite, Velocity, Lotter

Abstract
Accurately measuring Manning's roughness coefficient is crucial for enhancing the precision of hydraulic models and supporting informed decision-making in water resource management. Traditionally, this coefficient is determined using the cross-sectional mean velocity, which may introduce inaccuracies due to its approximate nature. However, estimating Manning's roughness coefficient through flow velocity distribution analysis remains a relatively underexplored approach. This study aims to improve the accuracy of estimating Manning's roughness coefficient by analyzing the velocity distribution at two vertical positions within the flow: z/H = 0.2 and z/H = 0.8. Secondary velocity data were obtained from four locations to support this investigation: a laboratory flume, the Selokan Mataram irrigation channel, the Kuning River, and the Opak River. The research methodology involves simplifying and applying analytical equations needed to determine Manning's roughness coefficient based on the velocity profile. The results indicate that, in natural river systems, Manning's roughness coefficient ranges from 0.035 to 0.095 at z/H = 0.8 and z/H = 0.2 and from 0.032 to 0.085 at z/H = 0.4 and z/H = 0.2.

INTRODUCTION

The Manning roughness coefficient is a crucial parameter in determining flow resistance, significantly influencing the accuracy of one-dimensional flow simulations. (Chengye et al., 2024). Precisely assessing Manning's roughness coefficient is essential for open channel analysis. (Mardi & Murmu, 2024). However, accurately determining this coefficient remains challenging due to its inherent uncertainty. (Pandey et al., 2024). A correct assessment of Manning's roughness coefficient improves the accuracy of hydraulic models and supports better decision-making in water resource management. (Bhargav et al., 2024).

Various methodologies have been developed to address these challenges and determine Manning's roughness coefficient. Ezzeldin & Abd-Elmaboud, (2024) Proposed an artificial intelligence (AI)-based approach using a recurrent artificial neural network (RANN) combined with the artificial hummingbird optimization algorithm (AHA). Similarly, Alrammahi, (2024) Estimated the coefficient by analyzing land cover changes from 2007 to 2023. Other methods, such as deep learning models utilizing long short-term memory (LSTM) neural networks Chengye et al., (2024) and computational modeling through HEC-RAS (Bhargav et al., 2024), have also been explored.

In addition to technology-based approaches, some studies have assessed the roughness coefficient based on physical characteristics. Amsie et al., (2024) examined the influence of coarse aggregate size while S.-Q. Yang & Tan, (2008) Investigated the effects of particle morphology on erosion and flow resistance. Similarly, S. Q. Yang et al., (2005) Analyzed the impact of bed roughness and geometry on total flow resistance in alluvial rivers. (Aberle & Smart, 2010) Further explored flow resistance values by evaluating hydraulic geometry and structural roughness in steep-slope flows. Moreover, roughness coefficients may vary depending on erosion control techniques. (Alvis et al., 2024).

Despite the numerous approaches to estimating Manning's roughness coefficient, assessments based on flow velocity distribution remain limited. Maini et al. (2024) calculated the coefficient using vertical velocity distribution at two locations within the inner region of the flow. In an open channel, the flow velocity profile consists of two primary regions: (1) the inner region near the channel bed, where velocity follows a logarithmic distribution, and (2) the outer region, which extends to the water surface and may deviate from the ideal logarithmic profile (Kironoto & Graf, 1994; Kironoto & Graf, 1995).

Maini et al., (2024) Manning's coefficient was estimated solely from velocity distribution sites within the inner region. In contrast, this study aims to expand on their work by evaluating the coefficient using velocity distribution measurements from both the inner and outer areas. While Maini et al., (2024) employed Lotter, (1933) Approach to determine the composite Manning coefficient, this study conducts a comparative analysis using the method proposed by (Einstein & Banks, 1950)

The Manning roughness coefficient is a crucial parameter in hydraulic modeling, especially for channel design, flood prediction, and water resource management. Accurately estimating this coefficient is essential, as even small errors can lead to inefficient designs, inaccurate flood forecasts, and suboptimal water management strategies. Traditionally, the Manning coefficient is estimated to use the cross-sectional mean velocity, which may lead to inaccuracies due to its approximate nature. Therefore, efforts to improve the accuracy of the Manning coefficient determination are ongoing.

Various methods have been developed to estimate this coefficient, including artificial intelligence (AI)-based approaches, computational modeling using HEC-RAS, and physical analysis of channel characteristics. However, each method has limitations: AI and modeling approaches usually require large and good-quality data sets, while physical analysis is often difficult to apply in non-uniform natural channels. In addition, the use of cross-sectional average velocities ignores local velocity variations that can significantly affect the accuracy of the estimation. (Sessions & Valtorta, 2006)

To address these challenges, recent studies have explored alternative approaches. Maini et al., (2024) For instance, the Manning coefficient was estimated to use vertical velocity distribution at two points in the inner region of the flow. While their study provides a valuable foundation, we argue that relying solely on measurements in the inner region may not adequately capture the complexities of natural or engineered channel flows. The velocity distribution approach, however, offers a more detailed and potentially accurate alternative to the conventional cross-sectional mean velocity method.

This research builds upon that premise by evaluating the Manning roughness coefficient using velocity distribution measurements taken from both the inner and outer regions of the flow ($z/H = 0.8$ & 0.2 and $z/H = 0.4$ & 0.2) across different channel types, including laboratory flumes, irrigation channels, and natural rivers. In addition, the study compares Lotter's composite method (1933), as employed by Maini et al., (2024), with the method developed by Einstein & Banks, (1950) To assess the consistency and reliability of each approach. This work aims to determine whether incorporating velocity data from inner and outer flow regions leads to more accurate Manning coefficient estimates and identify which composite method yields more consistent results under varying flow conditions.

RESEARCH METHODS

This study explores the application of vertical flow velocity distribution measurements at various depths to enhance the estimation of the Manning roughness coefficient. In their research, Maini et al. (2024) utilized velocity measurements at $z/H = 0.2$ and $z/H = 0.1$, focusing on the inner region of the flow. The present study expands the measurement approach to include inner and outer areas, specifically at $z/H = 0.8$ and $z/H = 0.2$.

The selection of these points is aligned with commonly adopted practices for estimating average flow velocity, such as using a single-point measurement at z = 0.4D from the channel bed or two-point measurements at z = 0.8D and z = 0.2D. In addition to evaluating the z/H = 0.8 and z/H = 0.2 pair, this study also examines the effectiveness of using velocity measurements at z/H = 0.4 and z/H = 0.2 for estimating the Manning coefficient.

Using velocity measurement points at z/H = 0.8 and z/H = 0.2 provides a practical advantage, as these two points can serve a dual purpose: estimating the vertical average velocity and simultaneously allowing for the determination of Manning's roughness coefficient. This dual function enhances efficiency and simplifies the measurement process in field and laboratory applications. This study uses secondary data from previous research conducted in various channels. The data were collected from four distinct sources: (1) laboratory flume experiments conducted by Andayono, (2003) and Nindito, (2003), (2) field measurements in an irrigation channel (Selokan Mataram) based on the research by Ikhsan, (2005), and (3) river flow data from the Kuning and Opak Rivers, as reported in studies by Giarto, (2016) and Kiptiah, (2016) studies. These datasets provide a diverse range of channel conditions—laboratory, irrigation, and natural rivers— essential for evaluating the performance and applicability of the Manning coefficient estimation methods under different flow environments.

This study employs two main analytical approaches. The first involves estimating the Manning roughness coefficient using two-point velocity distribution measurements based on the equation proposed by Maini et al., (2024) In combination with the conventional Manning equation. The second analysis refers to the classification of velocity distribution into flow regimes—smooth, transitional, and rough—following the formulation by Colebrook & White, (1938), as expressed in Equations 1 to 3. In these equations, u_* Denotes the shear velocity (m/s), u is the measured point velocity at a given depth (m/s), ν is the kinematic viscosity of the fluid (m²/s), and z represents the vertical distance from the channel bed (m).

The categorization relies on the relationship between these parameters and the flow characteristics, determining whether the flow regime is smooth, rough, or turbulent transition.

$$\frac{u}{u_*} = 5.75\ \log\left(\frac{104\,z}{\delta}\right)\ for\ \frac{u_*\,k_s}{\nu} \leq 5 \qquad (1)$$

$$\frac{u}{u_*} = 5.75\ \log\left(\frac{30\,z}{k_s}\right)\ for\ \frac{u_*\,k_s}{\nu} \geq 70 \qquad (2)$$

$$\frac{u}{u_*} = 5.75\ \log\left(\frac{30\,z}{\frac{2\delta}{7}+k_s}\right)\ for\ 5 < \frac{u_*\,k_s}{\nu} > 70 \qquad (3)$$

Maini et al., (2024) Formulated and analyzed Equation 3, resulting in an expression for calculating the Manning roughness coefficient based on two velocity measurements taken at different vertical positions within the flow. This formulation is presented in Equation 4. In this context, ξ represents the velocity ratio u_b/u_a, where u_b and u_a are the velocities measured at two specified depths.

Furthermore, this study employs Equations 5 and 6 to calculate the composite Manning roughness coefficient using the methods proposed by Lotter (1933) and Einstein & Banks (1950), respectively. These methods allow for the integration of local roughness effects across different subsections of the channel cross-section.

$$n_y/B = \frac{H^{1/6}}{\sqrt{g}\left(\frac{(5.75\log b+2.28)-\xi(2.28+\log a\ 5.75)}{(\xi-1)}\right)} \qquad (4)$$

$$n_c = \frac{PR^{5/3}}{\sum\frac{1}{n_i}R_iP_i^{5/3}} \qquad (5)$$

$$n_c = \left(\frac{1}{P}\sum_{i=1}^{i=N} P_i n_i^{3/2}\right)^{2/3} \qquad (6)$$

In addition to Equation 4, the study employs Manning, (1891) Equation, as illustrated in Equation 7. Where H = Flow depth (m), b = Upper z/H point, a = Lower z/H point, P = Wetted perimeter (m), R = Hydraulic radius (m), n_i = Segment Manning's coefficient, n_c = Composite Manning's coefficient, P_i = Segment wetted perimeter (m), R_i = Segment hydraulic radius (m), n = Manning (s/m$^{1/3}$), S = energy slope (m).

$$n = \frac{R^{\frac{2}{3}}\sqrt{S}}{u} \quad (7)$$

The analytical procedure begins with the acquisition of vertical flow velocity profile data. The collected data is screened and validated to ensure accuracy and reliability before further processing. Subsequently, flow resistance values are determined using two methodologies. The first method relies on velocity measurements at two vertical distribution locations. The second method employs Manning's equation with the average vertical velocity distribution data. Afterward, the flow resistance values are re-evaluated using the composite Manning equation *(n_c)*, as illustrated in Equations 5 and 6. The analysis of Manning's roughness coefficient is performed using Equation 7.

RESULTS AND DISCUSSION

Flow Velocity Distribution

In using equation 8 in determining the value of Manning's roughness, the vertical direction flow velocity data must be ensured to be by and follow the requirements of the logarithm theory. Flow velocity calibration was carried out in this study to ensure that all vertical direction flow velocity data were based on the logarithm theory. The suitability of the vertical direction flow velocity distribution can be seen by comparing the values of *ln z/k$_s$* and velocity *(u)* in this study. The results of checking the suitability and validity of the logarithm theory can typically be seen in Figure 1.

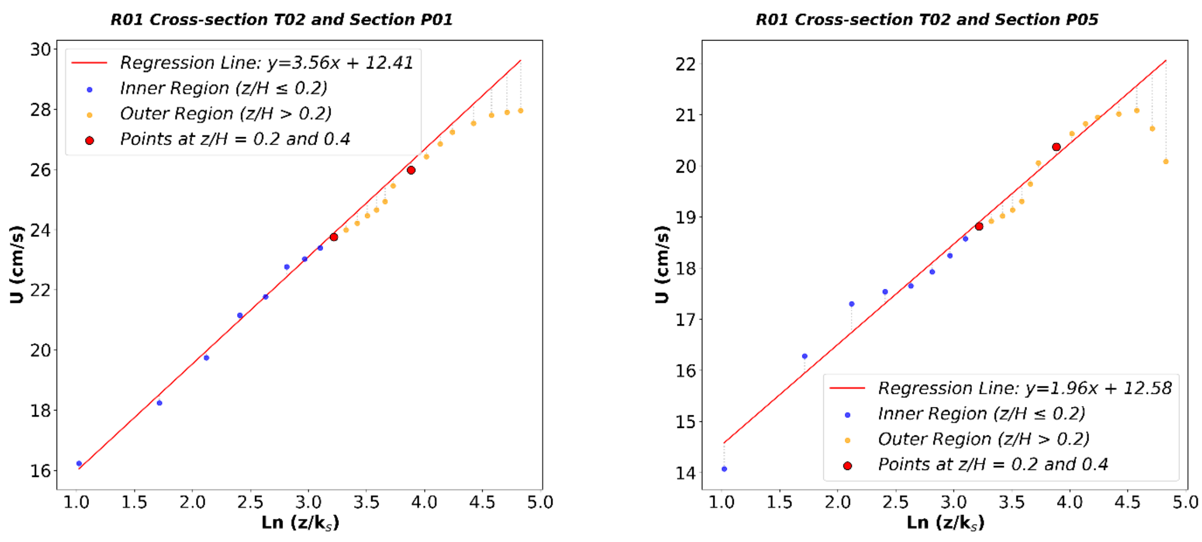

(a) (b)

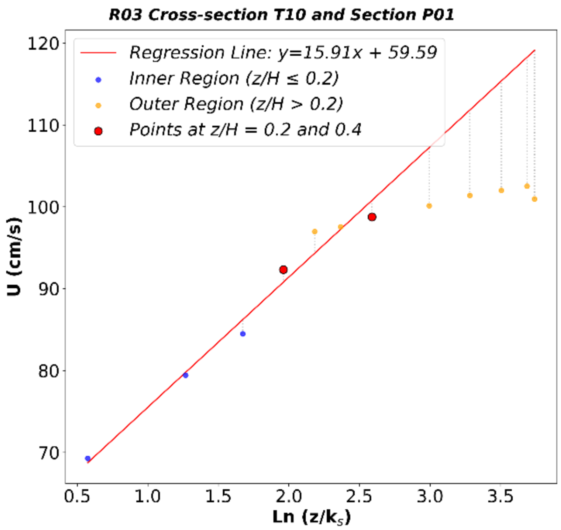

(c)

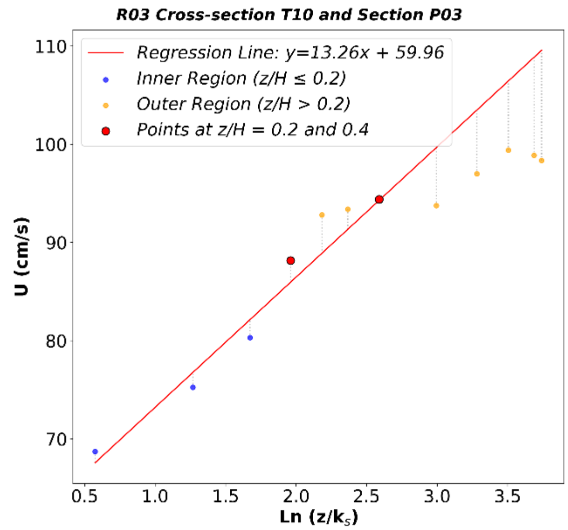

(d)

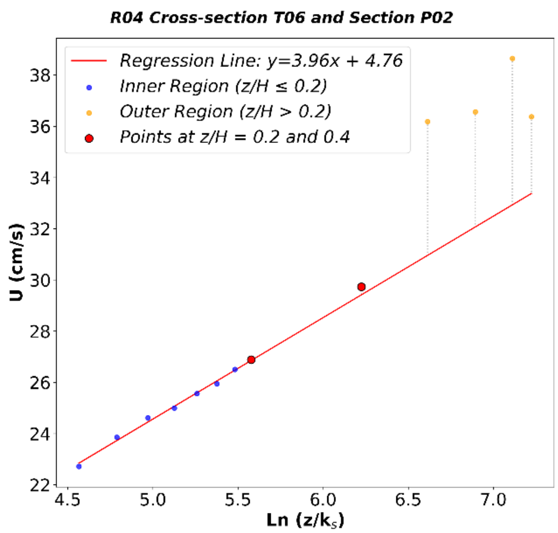

(d)

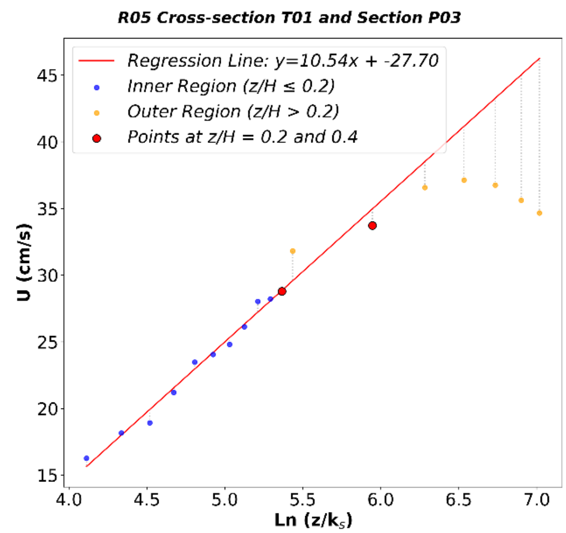

(e)

Figure 1. The typical results of the comparison between *ln(z/k$_s$)* and u for the data are as follows: (a & b) Laboratory data, both at the center and edge of the cross-section, (c & d) Selokan Mataram irrigation channel data, both at the center and edge of the cross-section, (e) Yellow River data, and (f) Opak River data.

All measurement data—from laboratory experiments, the Mataram irrigation channel, and natural river observations—exhibit a linear relationship in inner and outer regions. This indicates that the velocity distributions in all datasets conform to the logarithmic law, validating their suitability for use in Manning's roughness coefficient analysis.

As illustrated in Figure 1, the velocity values in the inner region consistently follow the logarithmic distribution across all datasets, including laboratories, artificial channels, and natural rivers. This consistency confirms that the inner region typically adheres to the log-law behavior. However, several data points deviate from the expected logarithmic distribution for the outer region, as shown in the figure. Therefore, these deviations must be considered when applying velocity values from the outer region to estimate Manning's roughness coefficient using Equation 4.

Such deviations from the logarithmic velocity distribution- above or below the expected trend—can introduce significant errors in determining Manning's roughness coefficient. An upward shift from the logarithmic trend results in an underestimated roughness coefficient, whereas a downward shift leads to an overestimation. This phenomenon is further demonstrated and discussed in detail in the following sections of this study.

Determination of composite Manning's method

Maini et al., (2024) Developed an equation to calculate Manning's roughness coefficient utilizing two vertical flow velocity measurements, namely at *z/H* 0.4 and *z/H* 0.2, as articulated in the subsequent equation.

$$n_y/B = \left(\frac{H^{1/6}}{\frac{-0.02-5.45\left(\frac{u_{0.4}}{u_{0.2}}\right)}{\left(\frac{u_{0.4}}{u_{0.2}}-1\right)}} \right) \quad (8)$$

A simplified version of Equation 4 is derived for *z/H* 0.8 and *z/H* 0.2 using the points *z/H* 0.8 and *z/H* 0.2, as presented in Equation 9.

$$n_y/B = \left(\frac{H^{1/6}}{\frac{5.40-5.45\left(\frac{u_{0.8}}{u_{0.2}}\right)}{\left(\frac{u_{0.8}}{u_{0.2}}-1\right)}} \right) \quad (9)$$

The composite Manning roughness coefficient is determined using the Lotter, (1933) and Einstein & Banks, (1950) Methods, henceforth referred to as the EDM method, as depicted in Figure 2, are based on Equations 8 and 9.

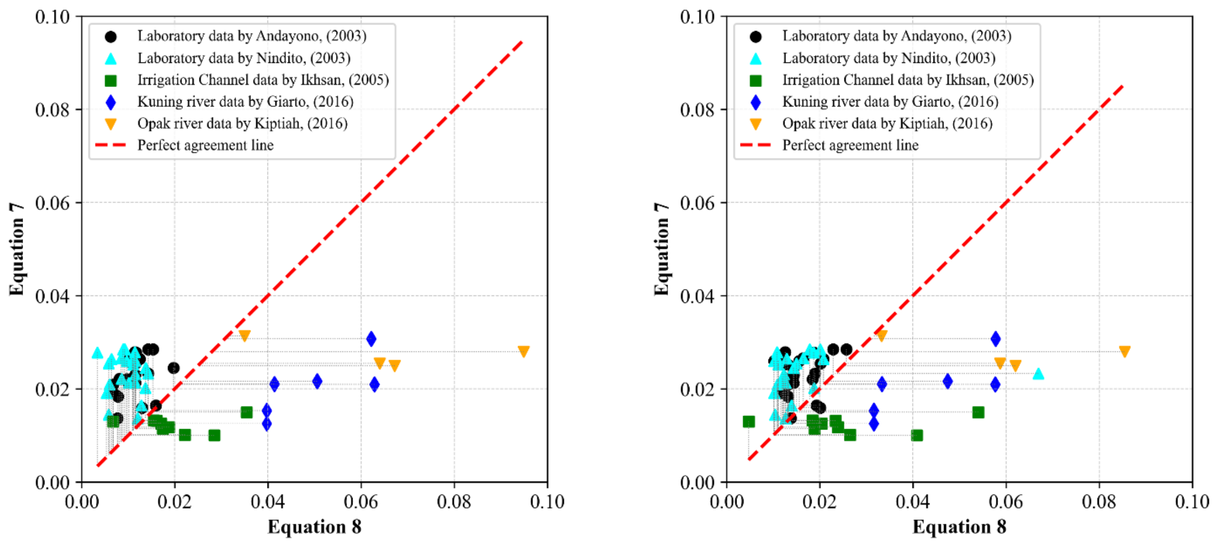

(a) (b)

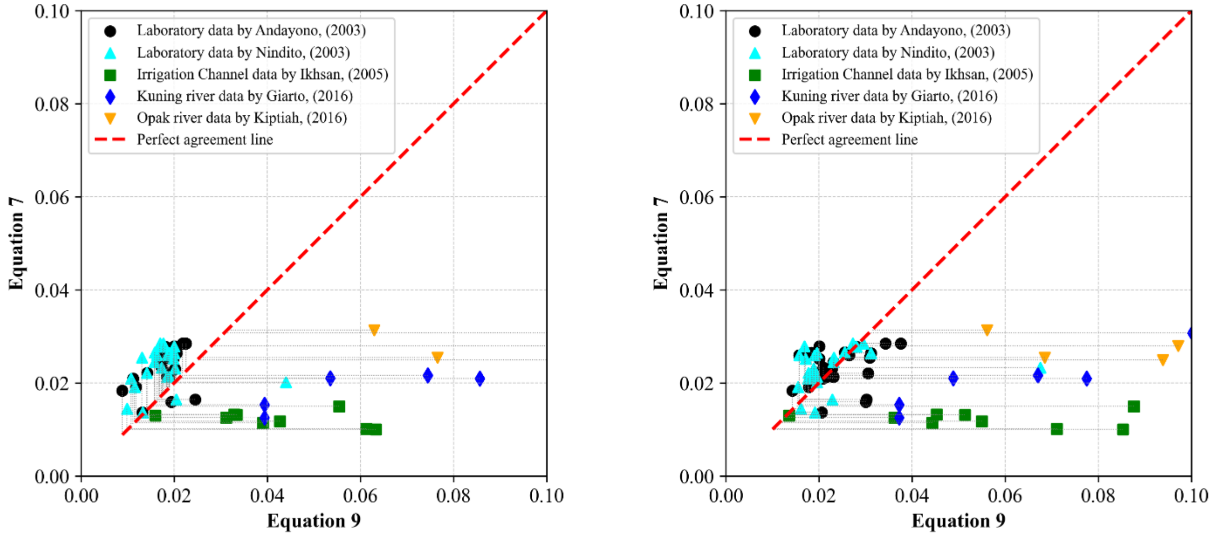

(c) (d)

Figure 2. Comparison of Manning's roughness coefficient values of equations 8 and 9 with equation 7 (a) Lotter method *z/H* 0.8 and *z/H* 0.2 (b) Lotter method *z/H* 0.4 and *z/H* 0.2 (c) EDM method *z/H* 0.8 and *z/H* 0.2 (d) EDM method *z/H* 0.4 and *z/H* 0.2.

According to Figure 2, the discrepancy of the composite Manning technique is evaluated from the roughness coefficient values derived from Equation 7. The minimal variation occurred in the Lotter method for points *z/H* 0.4 and 0.2, with an average deviation of 0.00005, whereas for points *z/H* 0.8 and *z/H* 0.2, the deviation was 0.0005. For the EDM approach, the deviation was 0.00008 at *z/H* 0.4 and 0.2 and 0.0005 at *z/H* 0.8 and *z/H* 0.2. The deviation was calculated by determining the difference between Manning's rough coefficient values obtained from Equations 8 and 9 and the perfect line of agreement. These differences were computed for all data points where Manning's coefficient was evaluated. Subsequently, statistical analysis was conducted by averaging the deviation values. The resulting average deviation indicates that all tested approaches are valid and accurate in estimating Manning's roughness coefficient. This result is consistent with K. Yang et al. (2005), who concluded that the Lotter and the Einstein & Banks (1950) or EDM methods are among the most precise techniques for composite Manning estimation.

Figure 2 presents the results of Manning's roughness coefficient calculations, revealing deviations from those obtained using Equation 7. These deviations are illustrated in Figures 2a to 2d, where several comparison points between the values derived from Equations 8 and 9 and those from Equation 7 deviate, shifting to the left of the perfect agreement line. A closer examination of Figures 2a to 2d shows that the majority of these deviations originate from field measurement data, including the Mataram irrigation canal (represented by green square markers), the Yellow River (blue dots), and the Opak River (yellow dots).

Figure 3, specifically the yellow square labeled number 1, highlights a data point in the calculation of Manning's roughness coefficient that exhibits a significant deviation, with a value of 0.0574. The deviation is calculated similarly to the average deviation; however, it is performed for a single point in this case. The deviation is determined by comparing Manning's coefficient at yellow square point 1 to the ideal value along the perfect agreement line.

This large deviation occurs because the calculation of Manning's roughness coefficient using Equation 8 incorporates velocity measurements at positions z/H = 0.4 and z/H = 0.2, which deviate from the expected logarithmic velocity distribution. This discrepancy in velocity values leads to an inaccurate estimation of the coefficient. Further evidence of this deviation is illustrated in Figure 4.

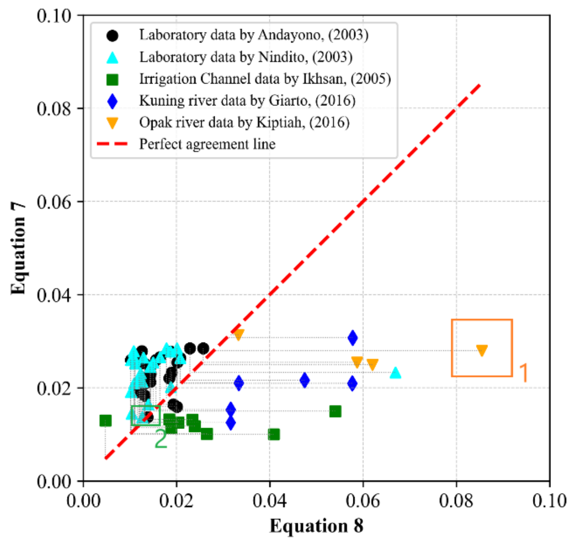

Figure 3. Evaluation of deviation of Manning's roughness coefficient results

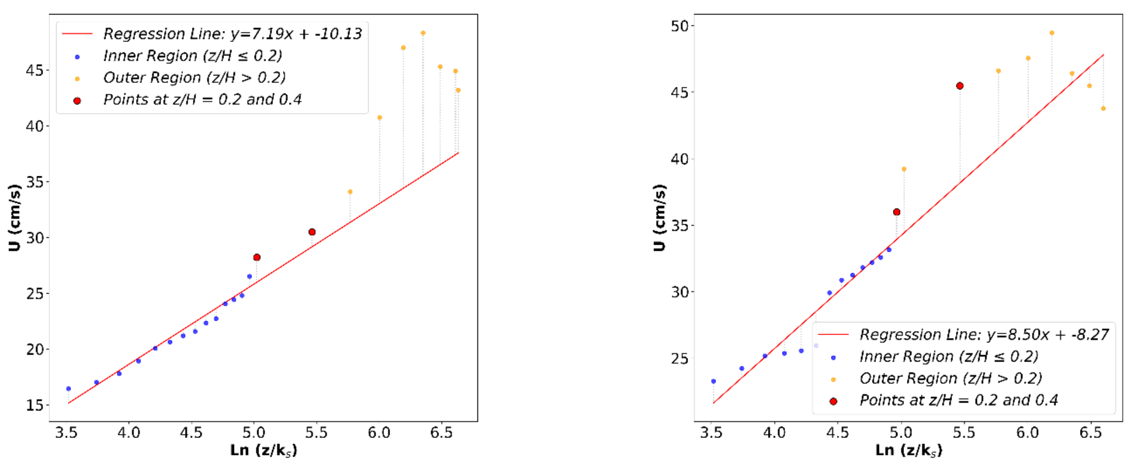

(a) (b)

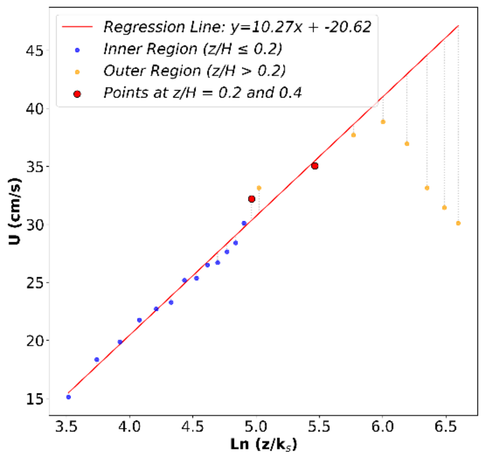

(c)

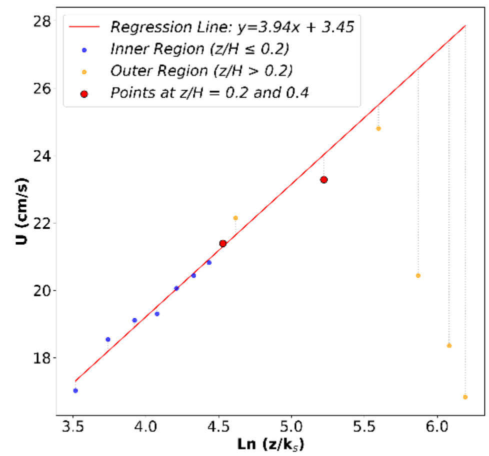

(d)

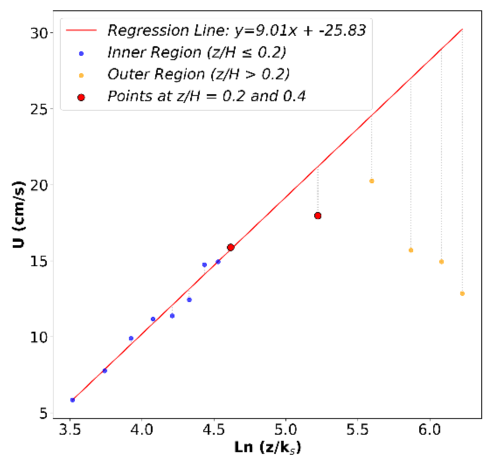

(e)

Figure 4. Logarithmic distribution of flow velocity in the river data resulting in deviated Manning's values (a) segment 1, (b) segment 2, (c) segment 3, (d) segment 4, and (e) segment 5.

The observed deviations at positions z/H = 0.4 and z/H = 0.2 from the logarithmic velocity distribution contribute to inaccuracies in calculating Manning's roughness coefficient. As shown in Figure 4a, the velocity at z/H = 0.2 deviates by 2.2406 cm/s, while the velocity at z/H = 0.4 deviates by 2.7473 cm/s from the corresponding logarithmic distribution values. Similarly, in segment 2 (Figure 4b), the velocity at z/H = 0.2 deviates by 4.8076 cm/s; at z/H = 0.4, the deviation reaches 7.3118 cm/s.

In segments 3 and 4, illustrated in Figures 4c and 4d, a deviation is found in one of the measured velocity points. Specifically, in segment 3, the velocity at z/H = 0.2 deviates by 2.2114 cm/s, while in segment 4, the velocity at z/H = 0.4 deviates by 0.7431 cm/s. A similar pattern continues in segment 5 (Figure 4e), where the velocity at z/H = 0.4 shows a significant deviation of 2.214 cm/s.

These consistent deviations in velocity measurements across multiple segments impact the accuracy of Manning's roughness coefficient calculation using Equation 4, which is derived from the flow velocity distribution formula proposed by Colebrook & White, (1938). As a result, the deviation in the calculated Manning's coefficient reached a value of 0.0574.

On the other hand, the green box labeled number 2 in Figure 3 shows a data point where Manning's roughness coefficient, calculated using Equation 8, closely matches the reference value, with a very small deviation of only 0.00005. This result contrasts with the yellow box (point 1), where a larger deviation was observed. As with the previous case, the deviation is calculated in the same manner as the average deviation, but it is evaluated for a single point in this instance. The comparison is made between the computed Manning's coefficient and the ideal value along the perfect agreement line.

To understand the accuracy of this result, a detailed examination of the logarithmic velocity distribution at *z/H* = 0.4 and *z/H* = 0.2 is essential. The velocity distribution patterns at these positions—used as the basis for Manning's coefficient calculation—are shown in Figure 5. This figure helps verify whether the velocity data at those depths adhere to the logarithmic distribution or exhibit deviations, which affects the precision of the resulting Manning's coefficient.

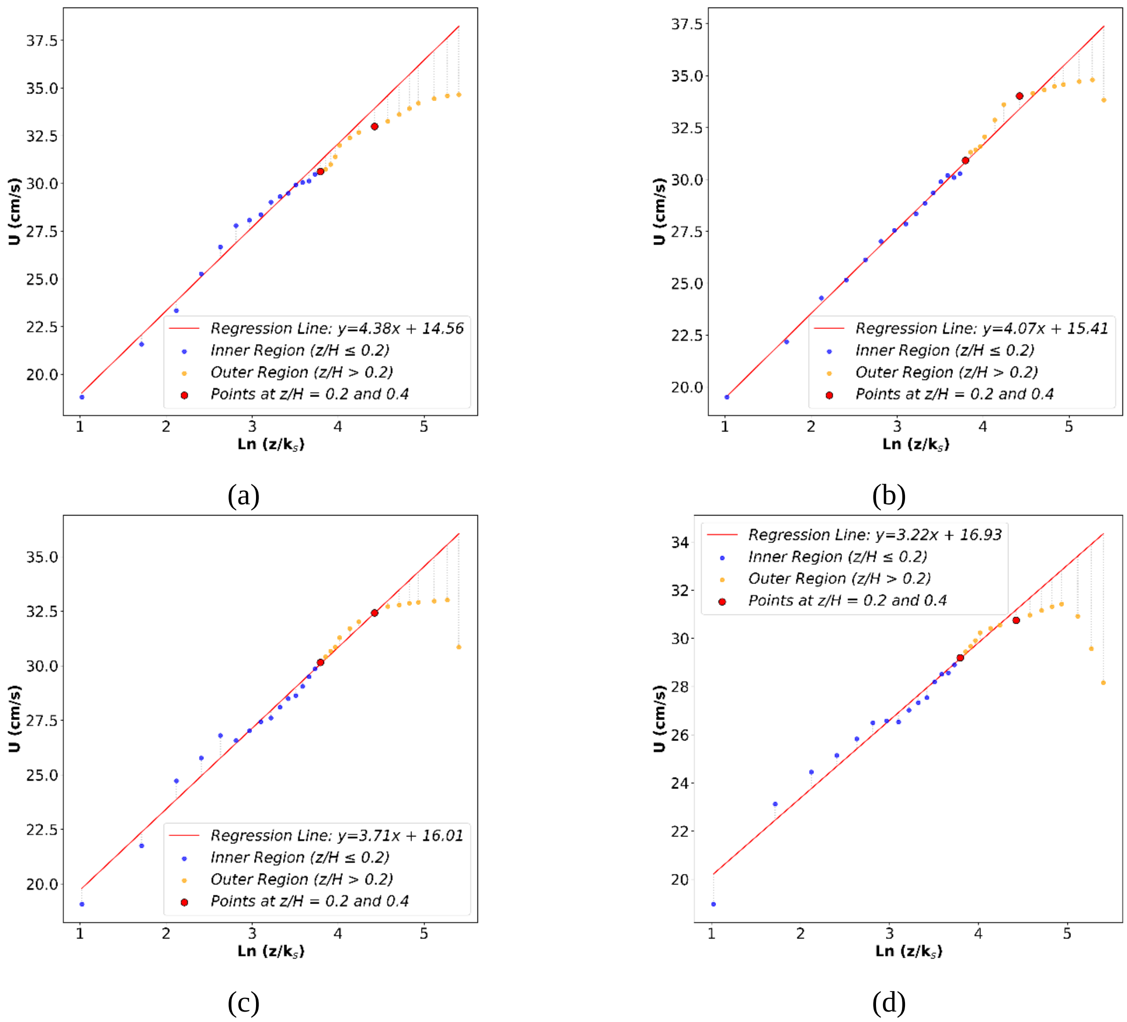

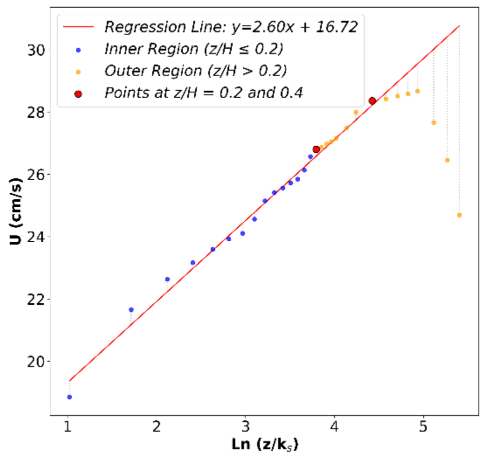

(e)

Figure 5. Logarithmic distribution of flow velocity in laboratory data resulting in deviating Manning's values (a) Segment 1 (b) Segment 2 (c) Segment 3 (d) Segment 4 and (e) Segment 5

The previous discussion has shown that large deviations of velocity values from the logarithmic distribution led to inaccuracies in estimating Manning's roughness coefficient. Figure 5 aims to validate the opposite scenario—whether minimal deviations in velocity from the logarithmic profile result in similarly accurate Manning's coefficient values.

Figure 5a indicates that the velocity values at z/H = 0.2 and z/H = 0.4 show small deviations of 0.5528 cm/s and 0.9480 cm/s, respectively. In segment 2 (Figure 5b), the velocity at z/H = 0.2 deviates by only 0.0872 cm/s, and at z/H = 0.4 by 0.1401 cm/s. Segment 3 (Figure 5c) also displays minimal deviations, with 0.0696 cm/s at z/H = 0.2 and 0.0110 cm/s at z/H = 0.4. Similarly, in segment 4 (Figure 5d), the deviation at z/H = 0.4 is 0.4304 cm/s. Segment 5 (Figure 5e) shows small deviations of 0.2222 cm/s and 0.1480 cm/s at z/H = 0.2 and z/H = 0.4, respectively.

Overall, the deviation values in these segments are predominantly below 1 cm/s. When Manning's roughness coefficient is calculated using Equations 8 and 9 based on these small deviations, the resulting deviation from the perfect line of agreement—shown in Figure 3—is only 0.00005. This confirms that the magnitude of velocity deviation from the logarithmic distribution directly affects the accuracy of Manning's roughness coefficient. The greater the deviation in velocity from the expected logarithmic trend, the larger the error in the estimated Manning's coefficient.

With an average velocity deviation of 3.1823 cm/s observed in the calculations presented in Figure 4, the resulting deviation in Manning's roughness coefficient reaches 0.0574. In contrast, the average velocity deviation shown in Figure 5 is significantly smaller, at 0.29 cm/s, corresponding to a much lower deviation in Manning's roughness coefficient, 0.00005. These results further reinforce the conclusion that the accuracy of velocity measurements relative to the logarithmic distribution directly impacts the precision of the calculated Manning's coefficient—larger deviations in velocity lead to greater errors in the resulting roughness coefficient.

As illustrated in Figure 2, the Manning roughness coefficient values for each location, derived from several composite Manning methods, yielded comparable findings, with detailed roughness coefficient values presented in Table 1.

Table 1. Manning's roughness coefficient results

Jenis Saluran	Metode lotter			Metode EDM		
	z/H 0.8 dan *z/H* 0.2	*z/H* 0.4 dan *z/H* 0.2	*z/H* 0.2 dan *z/H* 0.1	*z/H* 0.8 dan *z/H* 0.2	*z/H* 0.4 dan *z/H* 0.2	*z/H* 0.2 dan *z/H* 0.1
Lab	0.003 - 0.02	0.01 - 0.067	0.022 - 0.008	0.009 - 0.044	0.014 - 0.068	0.014 - 0.068
Irrigation Channel	0.007 - 0.035	0.005 - 0.054	0.049 - 0.024	0.016 - 0.063	0.014 - 0.088	0.014 - 0.088
River	0.035 - 0.095	0.032 - 0.085	0.069 - 0.029	0.039 - 0.114	0.037 - 0.1	0.037 - 0.100

Based on Table 1, all velocity point combinations, whether *z/H* = 0.8 and *z/H* = 0.2, *z/H* = 0.4 and *z/H* = 0.2, or *z/H* = 0.2 and *z/H* = 0.1—produce comparable ranges of Manning’s roughness coefficients across all data locations. This consistency holds regardless of whether the Lotter or EDM method is used. Therefore, it can be concluded that determining Manning’s roughness coefficient using two velocity measurement points, particularly at *z/H* = 0.8 and *z/H* = 0.2, as indicated in the equation, provides reliable and accurate predictions.

The findings of Maini et al., (2024), derived from two points at *z/H* 0.4 and *z/H* 0.2 using the Lotter composite Manning technique with laboratory data, ranging between 0.01 and 0.04. These results are comparable to our study's, which also showed similar ranges regardless of the *z/H* point combinations (0.8–0.2 or 0.2–0.1). Similarly, Rezaei Rad et al., (2024) Researched irrigation canals concerning soil texture, reporting Manning’s roughness coefficients between 0.017 and 0.083. These values also correspond to our results, which ranged from 0.016 to 0.063 using *z/H* points of 0.8 and 0.2. Additionally, Boyer, (1954) Evaluated Manning’s coefficient across 22 natural rivers in the Northwestern United States, using two velocity points (*z/H* 0.8 and 0.2) based on Equation 7, and found a coefficient range of 0.02 to 0.075. This aligns with our field data, where the roughness coefficient ranged from 0.035 to 0.095 using the Lotter method with similar point selection.

However, it is important to note that Manning’s roughness coefficient is highly sensitive to physical site conditions, such as channel shape, bed material, and vegetation. Therefore, while the alignment of numerical ranges may provide initial validation, it does not necessarily confirm the reliability or superiority of a specific method—especially when the dataset includes outliers or site-specific characteristics that are not adequately represented.

Based on the results presented in Table 1, Manning’s roughness coefficient derived from velocity distribution points at *z/H* 0.8 and *z/H* 0.2 demonstrates consistent applicability across various channel types—laboratory flumes, irrigation canals, and natural rivers. These points yield coefficient ranges comparable to other point combinations while maintaining a reasonable spread of values. Compared to the *z/H* 0.2 and 0.1 combinations, the *z/H* 0.8 and 0.2 pair demonstrates comparable stability and representativeness, particularly in natural channels with well-developed velocity profiles.

Notably, selecting *z/H* 0.2 and *z/H* 0.8 points offers a practical advantage. Beyond their ability to accurately estimate the Manning roughness coefficient, the velocity data from these two points can also be used to calculate the vertical mean velocity, a valuable parameter in hydraulic analysis. This dual functionality simplifies the field data collection process, reducing time and resource demands.

Given this practicality and the consistent range of values across diverse channel types, the *z/H* 0.8 and *z/H* 0.2 configuration can be considered the most effective and efficient approach for estimating Manning’s roughness coefficient using the Lotter or EDM method. However, as previously noted, the physical condition of each site and potential outlier influence must still be considered when interpreting these values.

CONCLUSION

This study demonstrates that the two-point vertical velocity measurement approach, specifically at relative depths of z/H = 0.8 and z/H = 0.2, is both a practical and reliable method for estimating Manning's roughness coefficient (n). The estimated n values derived from this configuration exhibit consistent ranges across various channel types: laboratory flumes (0.003–0.02), irrigation channels (0.007–0.035), and natural rivers (0.035–0.095) when applying the Lotter method. Comparable results were also obtained using the Einstein & Banks method (EDM), further supporting the robustness of the approach.

A comparison between the n values estimated via the two-point method (using Equations 8 and 9) and the reference values derived from the classical Manning equation (Equation 7) indicates that the smallest average deviation (0.00005) occurs when using the combination of z/H = 0.4 and 0.2 with the Lotter method. In contrast, z/H = 0.8 and 0.2 yields a slightly larger average deviation (0.0005), although still within acceptable accuracy thresholds.

Furthermore, the analysis reveals that significant deviations from the logarithmic law of vertical velocity distribution ($ln(z/k_s)$ versus u) can directly affect the accuracy of n estimation. For instance, a river segment exhibiting an average velocity deviation of 3.1823 cm/s corresponds to an n deviation of up to 0.0574. Conversely, laboratory conditions with a velocity deviation of less than 1 cm/s result in an n deviation as low as 0.00005. This highlights the crucial role of the validity of the logarithmic velocity profile, particularly within the inner flow region, in ensuring estimation accuracy.

In conclusion, the measurement configuration at z/H = 0.8 and 0.2 offers the most efficient balance between practicality and precision. In addition to yielding reliable estimates of n, it also facilitates the computation of depth-averaged velocity. However, verifying that the velocity measurements at these points conform to the logarithmic distribution, especially under field conditions characterized by flow heterogeneity, is essential to preserve estimation accuracy.

REFERENCES

Aberle, J., & Smart, G. M. (2010). The influence of roughness structure on flow resistance on steep slopes. *Journal of Hydraulic Research*, *41*(3), 37–41. https://doi.org/10.1080/00221680309499971

Alrammahi, F. S. (2024). Identification of the changes in Manning's coefficient for Erbil Basin using the ArcGIS, HEC-RAS, and remote sensing images. *AIP Conference Proceedings*, *3249*(1). https://doi.org/10.1063/5.0236579

Alvis, A. D., Luce, C. H., Istanbulluoglu, E., Black, T., Dieu, J., & Black, J. (2024). Using additional roughness to characterize erosion control treatment effectiveness in roadside ditch lines. *Earth Surface Processes and Landforms*, *49*(4), 1255–1272. https://doi.org/10.1002/esp.5763

Amsie, A. B., Ayalew, A. T., Mada, Z. M., & Finsa, M. M. (2024). Acclimatize experimental approach to adjudicate hydraulic coefficients under different bed material configurations and slopes with and without weir. *Heliyon*, *10*(11). https://doi.org/10.1016/j.heliyon.2024.e32162

Andayono, T. (2003). *Kajian lokasi pengambilan sampel terhadap penentuan debit sedimen suspensi rata-rata pada aliran dengan dan tanpa angkutan bed load* [Universitas Gadjah Mada]. https://etd.repository.ugm.ac.id/penelitian/detail/21729

Bhargav, A. M., Suresh, R., Tiwari, M. K., Trambadia, N. K., Chandra, R., & Nirala, S. K. (2024). Optimization of Manning's roughness coefficient using 1-dimensional hydrodynamic modelling in the perennial river system: A case of lower Narmada Basin, India. *Environmental Monitoring and Assessment*, *196*(8), 743. https://doi.org/10.1007/s10661-024-12883-w

Boyer, M. (1954). Estimating the manning coefficient from an average bed roughness in open channels. *Transactions, American Geophysical Union*, *35*(6), 957–961. https://doi.org/10.1029/TR035i006p00957

Chengye, L., Yang, P., Shiqi, L., Xianliang, Y., & Lishuang., Y. (2024). Roughness inversion method for river unsteady flow simulations based on deep learning. *Journal of Hydroelectric Engineering*, *43*(10), 42–52.

Colebrook, C. F., & White, C. M. (1938). Corrigendum. the Reduction of Carrying Capacity of Pipes With Age. *Journal of the Institution of Civil Engineers*, *9*(7), 1. https://doi.org/10.1680/ijoti.1938.14612

Einstein, H. A., & Banks, R. B. (1950). Fluid resistance of composite roughness. *Transactions, American Geophysical Union*, *31*(4), 603. https://doi.org/10.1029/TR031i004p00603

Ezzeldin, R., & Abd-Elmaboud, M. (2024). Modeling flow resistance and geometry of dunes bed form in alluvial channels using hybrid RANN–AHA and GEP models. *International Journal of Sediment Research*, *39*(6), 885–902. https://doi.org/10.1016/j.ijsrc.2024.08.002

Giarto, R. B. (2016). *DISTRIBUSI KONSENTRASI SEDIMEN SUSPENSI PADA SUNGAI ALAMI (Studi Kasus Sungai Opak dan Sungai Kuning Yogyakarta)* [Universitas Gadjah Mada]. https://etd.repository.ugm.ac.id/

Ikhsan, C. (2005). *Pengukuran distribusi kecepatan dan konsentrasi sedimen suspensi pada aliran seragam tampang segi empat Di Saluran Induk Mataram, Yogyakarta* [Universitas Gadjah Mada]. https://etd.repository.ugm.ac.id/

Kiptiah, M. (2016). *Distribusi Kecepatan Aliran Sedimen Suspensi pada Sungai Alami (Studi kasus sungai Opak dan sungai Kuning di Yogyakarta)* [Universitas Gadjah Mada]. https://etd.repository.ugm.ac.id/penelitian/detail/103480

Kironoto, B. A., & Graf, W. H. (1994). Turbulence characteristics in rough uniform open-channel flow. *Proceedings of the Institution of Civil Engineers: Water, Maritime and Energy*, *106*(4), 333–344. https://doi.org/10.1680/iwtme.1995.28114

Kironoto, B. A., & Graf, W. H. (1995). Turbulence characteristics in rough non-uniform open-channel flow. *Proceedings of the Institution of Civil Engineers: Water, Maritime and Energy*, *112*(4), 336–348. https://doi.org/10.1680/iwtme.1995.28114

Lotter, G. K. (1933). Considerations on hydraulic design of channels with different roughness of walls. *Transactions, All-Union Scientific Research Institute of Hydraulic Engineering, Leningrad*, *9*, 238–241.

Maini, M., Kironoto, B. A., Istiarto, & Rahardjo, A. P. (2024). Evaluating Manning's Roughness Coefficient for Flows with Equilibrium and Non-equilibrium Sediment Transport. *Jordan Journal of Civil Engineering*, *18*(1), 65–80. https://doi.org/10.14525/JJCE.v18i1.06

Manning, R. (1891). On the flow of water in open channels and pipes. *Ireland, Transactions of the Institution of Civil Engineers Of*, *20*, 161–207.

Mardi, M., & Murmu, S. K. (2024). An experimental study of Manning's roughness coefficient with an Acoustic Doppler Current Profiler (ADCP) method of the River Ganga at Gandhi-Ghat Site, Patna, India. *Journal of The Institution of Engineers (India): Series A*, *105*(4), 987–1001. https://doi.org/10.1007/s40030-024-00838-w

Nindito, D. A. (2003). *Kajian Pengambilan Sampel Sedimen Suspensi Rata-Rata Melalui Pengukuran 1, 2 Dan 3 Titik; Dan Pengaruhnya Terhadap Lokasi Pengambilan Sampel Arah Transversal*. Universitas Gadjah Mada.

Pandey, R., Jayanth, G. R., & Kumar, M. S. M. (2024). Enhancing Robust Control of Irrigation Canal Systems with Quantitative Feedback Theory (QFT). *2024 6th International Conference on Electrical, Control and Instrumentation Engineering (ICECIE)*, 1–8. https://doi.org/10.1109/ICECIE63774.2024.10815638

Rezaei Rad, H., Ebrahimian, H., Liaghat, A., Khalaji, F., & Shabani Arani, M. (2024). Temporal variation of

Manning roughness coefficient in furrow irrigation and its relationship with various field parameters. *Applied Water Sciences*, *15*(1), 1–19. https://doi.org/10.1007/s13201-024-02334-9

Sessions, V., & Valtorta, M. (2006). The effects of data quality on machine learning algorithms. *Proceedings of the 2006 International Conference on Information Quality*, *ICIQ 2006*, *132*(January), 102549. https://doi.org/10.1016/j.is.2025.102549

Yang, S.-Q., & Tan, S.-K. (2008). Flow Resistance over Mobile Bed in an Open-Channel Flow. *Journal of Hydraulic Engineering*, *134*(7), 937–947. https://doi.org/10.1061/(asce)0733-9429(2008)134:7(937)

Yang, S. Q., Tan, S. K., & Lim, S. Y. (2005). Flow resistance and bed form geometry in a wide alluvial channel. *Water Resources Research*, *41*(9), 1–8. https://doi.org/10.1029/2005WR004211